STRUCTURAL AND ELECTRONIC PROPERTIES OF TRANSITION METAL DI-CHALCOGENIDES (MX_2) M=(Mo, W) AND X=(S, Se) IN BULK STATE: A FIRST-PRINCIPLES STUDY

Ram Prasad Sedhain and Gopi Chandra Kaphle

Journal of Institute of Science and Technology

Volume 22, Issue 1, July 2017

ISSN: 2469-9062 (print), 2467-9240 (e)

JIST, **22** (1): 41-50 (2017)

Published by:

Institute of Science and Technology

Tribhuvan University

Kirtipur, Kathmandu, Nepal

JIST 2017, 22 (1): 41-50
ISSN: 2469-9062 (p), 2467-9240 (e)

Research Article

STRUCTURAL AND ELECTRONIC PROPERTIES OF TRANSITION METAL DI-CHALCOGENIDES (MX_2) M=(Mo, W) AND X=(S, Se) IN BULK STATE: A FIRST-PRINCIPLES STUDY

Ram Prasad Sedhain[1], and Gopi Chandra Kaphle[2, 3, *]
[1]*Patan Multiple Campus, Tribhuvan University, Lalitpur, Nepal*
[2]*Central Department of Physics, Tribhuvan University, Kirtipur, Nepal*
[3]*Hydra Research Centre for Basic and Applied Sciences, Kathmandu, Nepal*
**Corresponding E-mail: gck223@gmail.com*

ABSTRACT

Transition metal di-chalcogenides (MX_2) M=(Mo, W) and X=(S, Se) in bulk state are of great interest due to their diverse applications in the field of modern technology as well as to understand the fundamental aspect of Physics. We performed structural and electronic properties of selected systems using density functional theory implemented in Tight Binding Linear Muffin- tin Orbital (TBLMTO) approach with subsequent refinement. The structural optimization is performed through energy minimization process and lattice parameters of optimized structures for MoS_2, $MoSe_2$, WS_2 and WSe_2 are found to be 3.20Å, 3.34Å, 3.27Å and 3.34Å respectively, which are within the error bar less than 5% with experimental values. The band gaps for all TMDCs are found to be of indirect types with semiconducting behaviours. The values of band gap of MoS_2, $MoSe_2$, WS_2 and WSe_2 in bulk state are found to be 1.16eV, 108eV, 1.50eV and 1.29eV respectively which are comparable with experimental and previously calculated data. Due to the symmetric nature of up spin and down spin channels of Density of States (DOS) all the systems selected are found to be non magnetic. However it fully supports the results obtained from band structure calculations. The potential and charge distributions plots support the results. The charge density plots reveals the covalent nature of bond in (100) plane. However (110) plane shows mixed types of bonding.

Keywords: Metal di-chalcogenides, TBLMTO approach, Electronic properties, Band gap, Density of states.

INTRODUCTION

Transition metal di-chalcogenides with generalized formula MX_2 where, M stands for Transition metals and X stands for chalcogen (Lee & Zuttel, 2003; Kasowski, 1973) have a large group of compounds and their electronic properties ranges as semiconducting, metallic and superconducting (Geim & Grigorieva, 2013; Wilson and Yoffe, 1969). In this communication we have used M = (Mo, W) and X = (S, Se) to know the behaviour these compounds in bulk states.

Werner Fischer (2001) proposed the term "chalcogen" when he worked in the group of Wilhelm Biltz at the University of Hannover, to denote the elements of group 16: Sulphides, Selenides and Tellurides (Fisher *et al.*, 2010). Then after, many researcher and investigator are interested on the field of transition metal di-chalcogenides because of their unique structure and verity of properties and diverse field of applications. The bulk state of transition metal dichalcogenides (TMDCs) formed by interacting the layers with Van der Waals forces, similar as hexagonal boron nitride and Graphene, so they are weakly bonded and has low shear resistance (Shankari *et al.*, 2008). Because of low shear resistance they are used as advanced applications like solid state lubricants, solar energy conversion, solar control coating, microelectronic devices, catalysts, and optical fibre and laser sources (Rasch *et al.*, 2007; Reshak and Auluck, 2003).

Mostly found MX_2 types of materials are achieved in different poly types, 1T, 2H, and 3R, depending upon the stacking pattern of consecutive layers of X-M-X sandwiching along the hexagonal c –axis, where the letters T, H, and R denote triagonal, hexagonal, and rhombohedral symmetries respectively (Coehoorn *et al.*, 1987). Both structural

and chemical forms of MX_2 under ambient conditions have been studied extensively with symmetry space group P63/mmc and unit cell $2H_c$-hexagonal structure (Aksoy *et al.,* 2006). Most of the works have been performed on the monolayer TMDCs because of their wide applications resemblance with Graphene, only few works on bulk with conflict results (Dean *et al.*, 2010; Coehoorn *et al*., 1987). This conflict results and lack of systematic study motivated us to study the structural and electronic properties of TMDCs in bulk state to explore the behaviour in more details.

There are more than sixty TMDCs are predicted till date out of them two thirds are assuming layered structure with varying electronic and magnetic properties. Due to the variety of the electronic and optical properties of TMDCs they show wide range of the band gaps ranging from insulator (HF_2) (Dean *et al.,* 2010) to semiconductor (MoS_2) (Radisavlijevice *et al.,* 2011; Fang *et al.,* 2012) to metallic (NbS_2) (Dean *et al.,* 2010), depending upon the type of poly types and the number of d electrons. In particular, TMDCs compounds based on molybdenum and tungsten have great interests due to their semiconducting behavior, they have wide band gaps ranging from visible to near infrared regions (Lee *et al.,* 2004; Mogne *et al.,* 1994). Group VI TMDs (e.g. MoS_2) are nominally semiconducting due to their fully filled lowest lying d-band. MoS_2 shows an indirect band gap semiconductor in its bulk form, which becomes a direct band gap semiconductor when we go from bulk to monolayer (Mak *et al*., 2010; Zhang *et al.,* 2014). During the process of desulfurization of crude oil in refineries we may used MoS_2 and WS_2 are as catalysts (Arslan *et al.,* 2004). Many works have been previously performed on ordered binary alloys (Pandey *et al.,* 2014; Poudel & Kaphle, 2016), ternary alloys (Lamichhane *et al.,* 2014), disorderedalloys (Kaphle *et al.,* 2012; Pal *et al.,* 2012; Kaphle *et al.,* 2016) and the cubic perovskites using Tight Binding Linear Muffin-tin Orbitals Atomic Sphere Approximations (TB-LMTO-ASA).

In this communication, we are going to explore the structural and electronic properties in Mo and W based dichalcogenides in bulk state using TB-LMTO-ASA approach.

COMPUTATIONAL METHOD

Present calculations are based upon the first principles approach, which involves the calculation of total ground state energy of the system considered through which we calculate lattice parameter of most stable structure. There are many first principles calculation methods (Kaphle *et al.,* 2012; Agrawal and Prakash, 2010) to evolved quantum mechanical formalism and were refined time to time to get better possible results. We used Density Functional Theory (DFT) (Par and Yang, 1986; Perdew and Kurth, 2003; Perdew *et al.,* 1996) based Tight Binding Linear Muffin-tin Orbital atomic sphere Approximation (TB-LMTO-ASA) approach (Skriver, 1984; Anisimov *et al.,* 1997) for the calculation of electronic and magnetic properties of ordered system. TBLMTO-ASA works on minimal basis set with the direct application of partial wave potential. In this approach, the solution to the Kohn Sham equations (Kohn and Sham, 1965) are performed self-consistently, and the augmented plane wave plus local orbital basis set is incorporated to represent the electronic band structure for all atoms and their corresponding orbitals. Throughout the calculation, we used local density approximation (LDA) exchange correlation potential (Kaxiras, 2003). The integration is performed in reciprocal space with 108 spatial k-points in the irreducible wedge of the Brillouin zone such that the core states are treated fully relativistically while the semi-core and valence states are treated semi-relativistically with default value of K_{cut} and E_{cut}. Finally all the calculations were iterated to self-consistency within the accuracy of 10^{-6} Rydberg through code.

RESULTS AND DISCUSSION

A. Structural Analysis and Lattice Parameters

The structural optimization is performed through energy minimization process taking base as a experimental value of lattice parameter. The structural positions for MX_2 are taken from Reshak and Auluk (2007) having positions M = (1/3, 2/3, 1/4), X_1 = (1/3, 2/3, z), X_2 = (2/3, 1/3, z-1/2) with hexagonal structure consisting of X-M-X layers belonging to $p6_3/mmc$ space symmetry. The space group number is 194 having the crystal structure hp_6.

The figure 1 (a and b top) show the energy verses lattice parameter of MoS_2 and $MoSe_2$ with optimized crystal structure through first principles study in figure 1 (c, d middle) and layered bulk structure with 3×2×1 super cell. From the figure the lattice parameter of most stable structure of MoS_2 and $MoSe_2$ are found to be 3.20Å and 3.34Å which are deviated less than 5% than experimental value. That may be due to the experimental set up environment and first principles approximation.

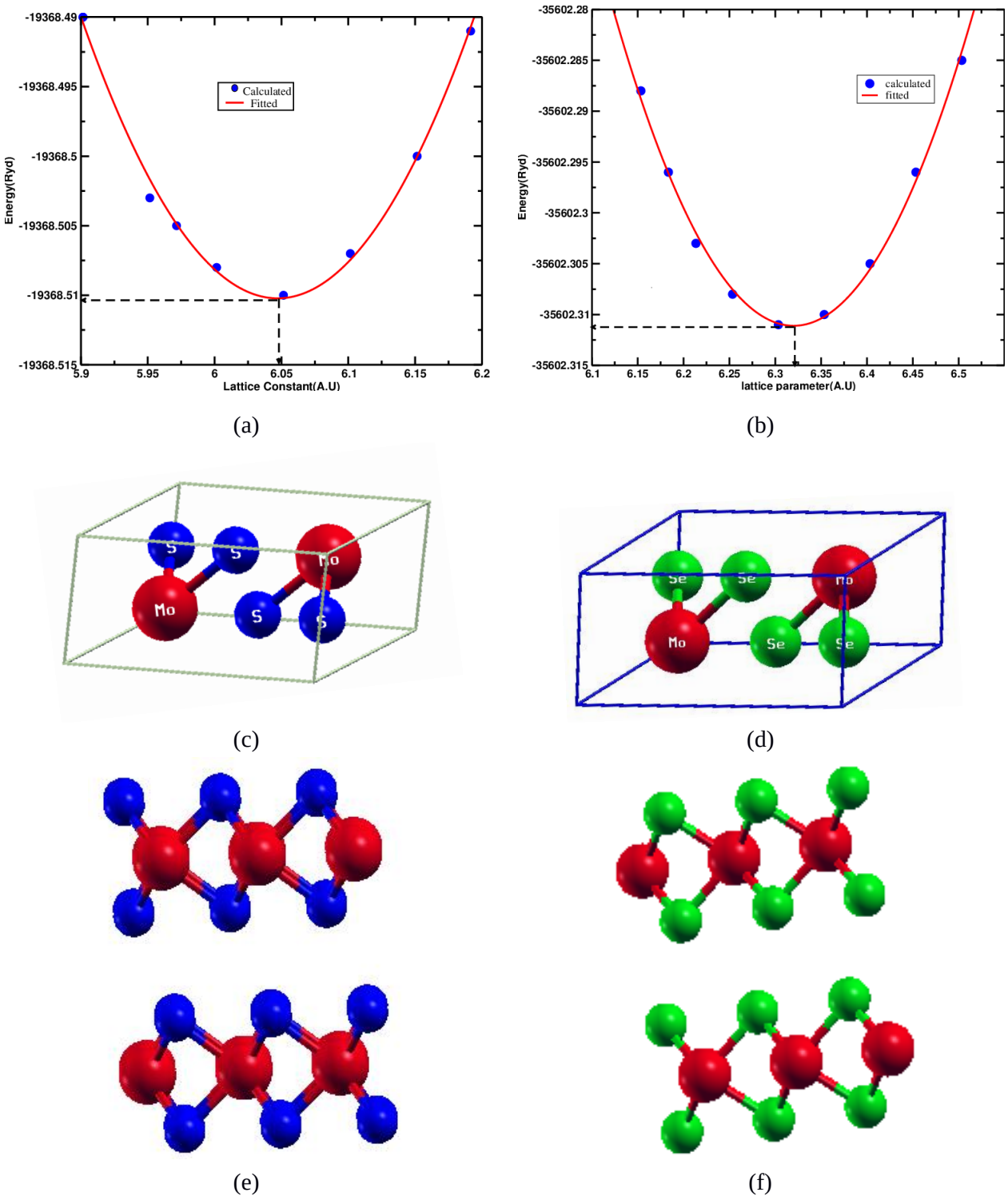

Fig. 1. (colour online) Plot of [top] energy vs lattice parameter (a, b), [middle] primitive Unit cell (c, d) and 3×2×1 super cell showing layered structure (e, f) for MoS_2 and $MoSe_2$ respectively.

Similarly the optimized lattice constant for WS_2 and WSe_2 are found to be 3.24Å and 3.34Å respectively. The calculated lattice parameter of WSe_2 is deviated around 5% than the experimental value where as this deviation is around 2% in WS_2. The energy minimization curve along with primitive unit cell and super cell are shown in figure 2 (a, b, c, d, e, f).

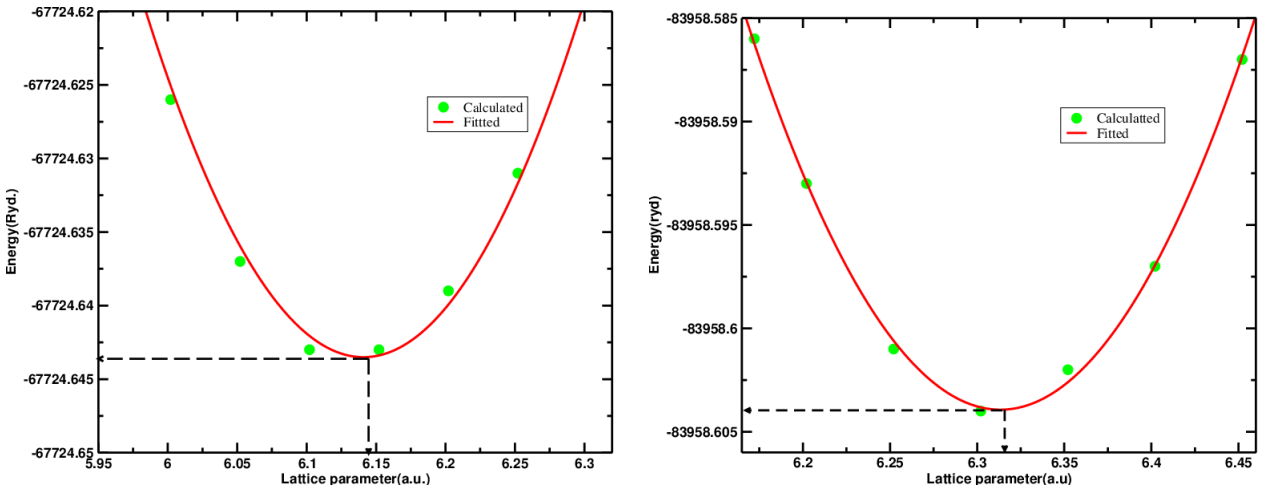

(a) (b)

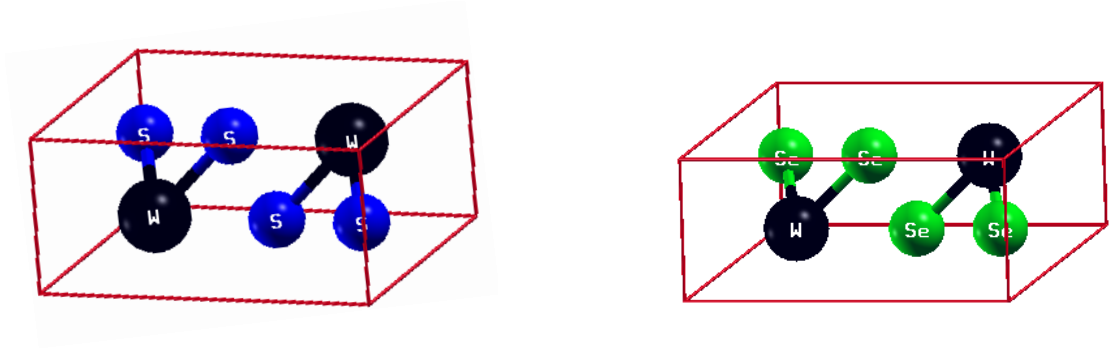

(c) (d)

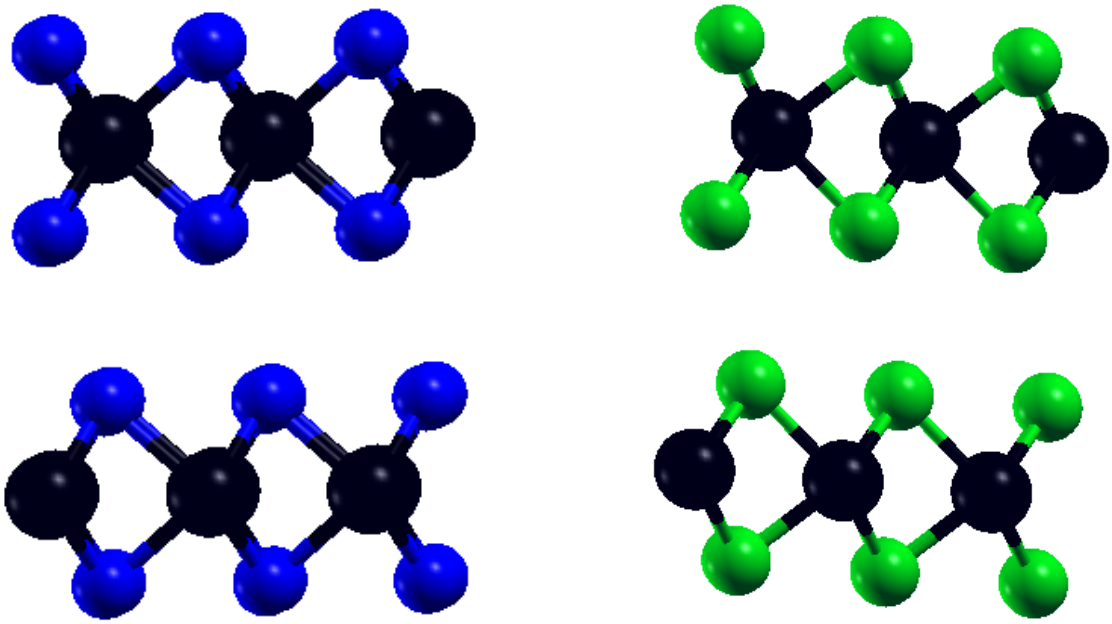

(e) (f)

Fig. 2. (colour online) Plot of [top] energy vs lattice parameter (a, b), [middle] primitive Unit cell (c, d) and 3×2×1 supercell showing layered structure (e, f) for WS_2 and WSe_2 respectively.

Table 1. Comparisons of lattice parameter of bulk MX_2 where M=(Mo, W and X=S, Se) from Present calculation and experimental value.

Properties	Bulk MoS_2	Bulk $MoSe_2$	Bulk WS_2	Bulk WSe_2
lattice constant (a) (Å)	3.20 **(present)** 3.16 (Wilson & Yoffe, 1969)	3.34 **(present)** 3.29 (Booker *et al.*, 2001)	3.24 **(present)** 3.15 (Schuttle *et al.*, 1987)	3.34 **(present)** 3.15 (Schuttle *et al.*, 1987)
c/a ratio	3.89 **(present)** 3.89 (Wilson & Yoffe, 1969)	3.90 **(present)** ——	3.92 **(present)** -------	3.90 **(present)** ------

B. Electronic Band Structure and Density of States Analysis

The band structure plot gives the idea that how energy eigen values behaves within high symmetry points of brillouin zone. The band structure directly affects the optical and electric properties of the materials, and hence very important to calculate the practicable optical excitation which determines the reflectivity, colour and dielectric reaction of the solid. By the help of band structure one also can determine the miscellaneous thermodynamic and mechanical properties.

The number of states per unit occupied energy level is called density of states. It also measures the number of allowed quantum states per unit energy range. To know the optical, electronic and magnetic properties of solids like as paramagnetic susceptibility, specific heat and various transport phenomena like density of states is the important parameter (Wilson & Yoffe, 1969; Boker *et al.*, 2001).

We have calculated band structure and corresponding partial DOS for every system under study. Figure 3 (a, b) represents total electronic band structure and corresponding partial density of states of MoS_2 and $MoSe_2$ in bulk state. Third panel of the figure (3a) represents the total band structure for MoS_2. From figure, it is clearly seen that Valence Band Maxima (VBM) lies at Γ- symmetric points and Conduction Band Minima (CBM) is in between Γ-point and K-points indicating that the type of band gap is indirect in nature and found to be 1.16eV. First and second panels of the figure 3 (a) represent partial density of state for spin up and fourth and fifth panels of figure 3 (a) represent the density of state for spin down state. The nature of PDOS for up and down spin channels are symmetric showing that MoS_2 is non magnetic in nature.

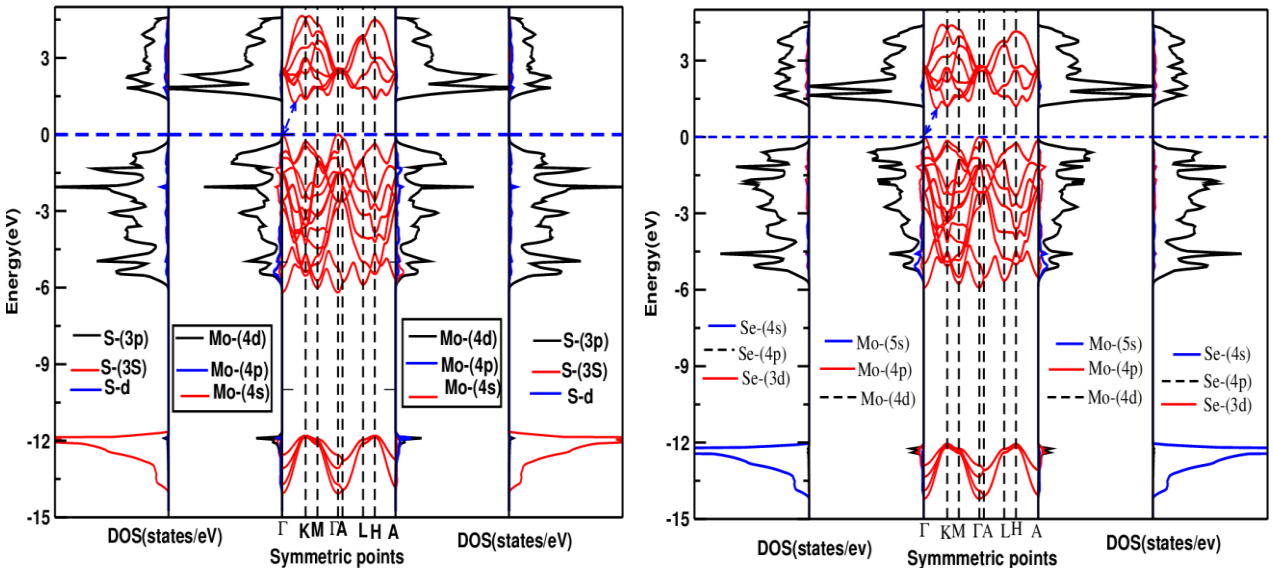

(a) (b)

Fig. 3. (colour online) Comparative study of PDOS and band structure of (a) MoS_2 and (b) $MoSe_2$.

From the comparative study of band structure and density of states it is observed that there are three different sets separated by certain gaps in band structure. First set of bands and density of States are seen around –11.8eV to -14eV energy range which are mainly due to the contribution of (3s) orbital of S atom. Another set of bands and density of states are found just below the Fermi level separated by the large gap from first set i. e. spreading within the energy range 0eV to -6eV. The main contribution of this set is due to strong hybridization of (4d) orbital of Mo atom and (3p) orbital of S atom and third set of bands and density of states lies above the Fermi level spreading within +1.0eV to +4.0eV energy range which arises due to the main contribution of (4d) orbital of Mo atoms. The contribution of (4p) orbital in down spin channel has negligible effect in band formation of this layer. Thus, it is clearly seen that the bands and states of density on up spin and down spin channel of band gap derived mainly from (4d) states of Mo and (3p) states of S.

Similarly, figure 3(b) represents the electronic band structure and corresponding density of states of ($MoSe_2$) in bulk state. The natures of layers are same as MoS_2 on which VBM lies in Γ- point and CBM lies between Γ-point and K-points, showing MoSe2 has indirect types of band gap with value 1.08eV. The second and third layers have same kinds of nature however, first layer shifted little a bit lower than MoS_2. The indirect band gap arises mainly due to the contribution of strong hybridization of (4d) orbital of Mo atom and (4p) orbital of Se atom.

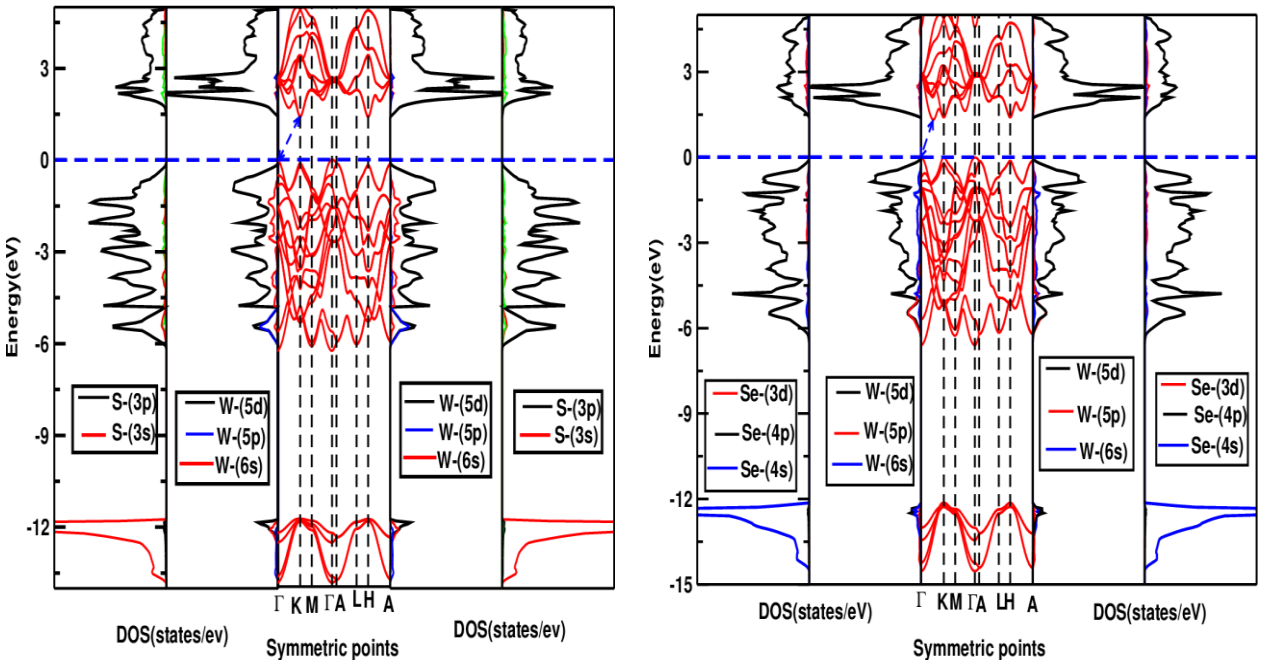

(a) **(b)**

Fig. 4. (colour online) Comparative study of PDOS and band structure of (a) WS_2 and (b) WSe_2.

The properties of WS_2 are more or less same as MoS_2 which has indirect in nature with band gap 1.40eV showing semiconducting properties. The band gap contribution is due to hybridization of (5d) states of W and (3p) states of S. The nature of WSe_2 and $MoSe_2$ resembles but the energy level span is slightly higher than WS_2 and $MoSe_2$. In case of WSe_2 the band gap arises due to hybridization of (5d) states of W and (4p) states of Se. The observed band gap is of indirect type with 1.27eV. The band gap variation with PDOS curve for both WS_2 and WSe_2 are shown in figure 4. The symmetric behaviour of up spin and down spin channel of DOS indicates that these materials bear non magnetic nature in bulk state.

The calculated band gap variations in MX_2 where M = (Mo, W) X = (S, Se) in the bulk state is shown in figure 5. The comparison of band gap to experimental as well as previously calculated results is tabulated in table 2.

Table 2. Comparison of band gap of bulk MX_2 where M=(Mo, W) X=(S, Se) calculated from present calculation with experiment and others.

Materials (Bulk State)	Band gap [eV] (Present)	Band gap [eV] (experimental)	Band gap[eV] (Previous Theoretical)
MoS_2	**1.16**	**1.23 (**Mak *et al.*, 2010) **1.29** (Boker *et al.*, 2001)	**1.15** (Mattheiss, 1973)
WS_2	**1.50**	**1.35 (**Schutte *et al.*,1987) **1.39 (**Gujarathia *et al.*, 2005**)**	**1.29** (Sharma *et al.*, 1999)
$MoSe_2$	**1.08**	**1.09** (Boker *et al.*, 2001)	**1.09** (Kumar *et al.*, 2015)
WSe_2	**1.29**	**1.20 (**Schutte *et al.*,1987**)** **1.30** (Finteis *et al.*,1997)	**1.13** (Kumar *et al.*, 2015)

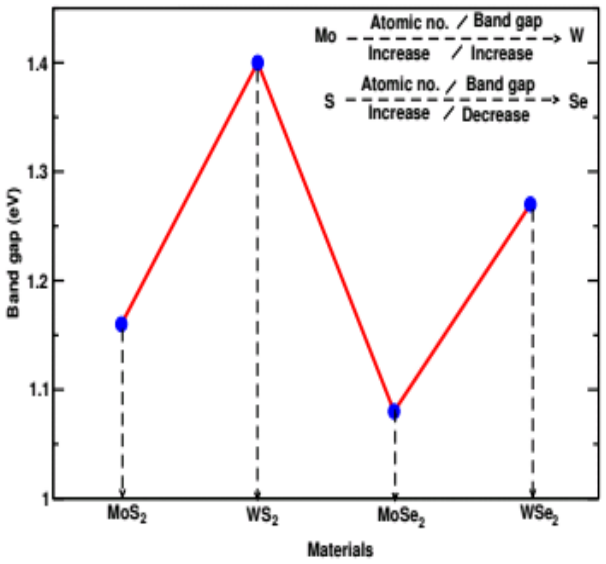

Fig. 5. Varation of band gap in MX_2.

From the figure it is found that the band gap of TMDCs is found to be increases as the atomic number of transition metal increases. Similarly the band gap of TMDCs is found to be decreases as the atomic number of Chalcogens increases.

C. Potential distribution and Charge density analysis

The distribution of potentials is considered as muffin tin potential in which potential is maximum near the core of atom and almost flat in the interstitial space which is resemblance with the charge density plot. From the charge distribution plot, it has been found that local maxima of the electronic charge is at position of the nuclei shown by high pick the distribution of charges is negligible i. e constant or flat in interstitial sites Both calculations are supporting with each other shown in figure 6. Same kinds of nature is observed in $MoSe_2$, WS_2 and WSe_2 respectively.

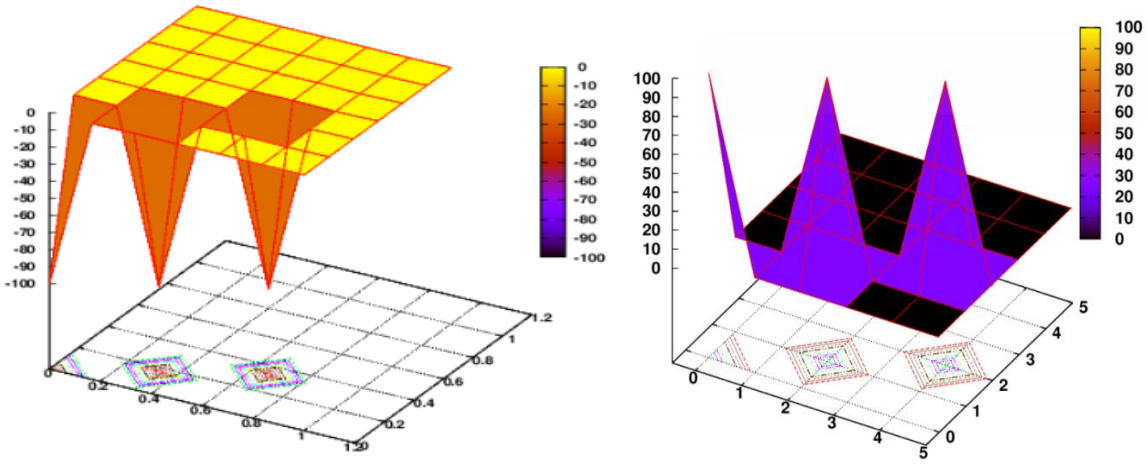

Fig. 6. (color online) Hartee potential and charge distribution Plot for MoS_2.

The nature of bond formation can be analysed through the charge density plot. If there is large accumulation of charge between two atoms, then covalent bond is established between these atoms. For the covalent nature between two atoms we can see the co-existence of the same contours in both atoms. The distribution of charge at (100) and (110) plane for MoS_2 are shown in figure 7.

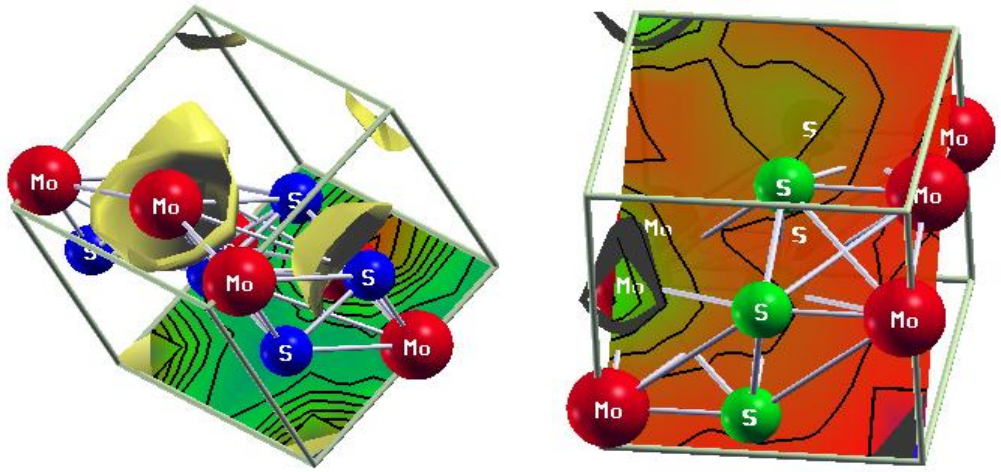

Fig. 7. (color online) Charge distribution plot at (100) and (110) plane .

From the figures, it is observed symmetric nature of charge distribution on the contours becomes symmetrically circular and for Mo-S (M-X) indicating covalent nature of bond between (M-X). In110 plane we observed contours which are not symmetric in nature. The symmetric and circular contours formed the covalent bond between the atoms and the non-symmetric and non-circular contour formed complex type of interaction which is difficult to predict the nature of bond may be assumed as mixed type. The nature of bond between (X-X) is found to be Van der Wall's type.

CONCLUSION

We performed energy minimization process to calculate the optimized structure of transition metal di-chalcogenides (MX_2) where, M=(Mo,W) and X=(S, Se) in Bulk state. From the calculations, the lattice parameter of MoS_2, $MoSe_2$, WS_2 and WSe_2 are found to be 3.20Å, 3.33Å, 3.24Å and 3.34Å which are closely related to experimental and other previously calculated results (less than 3% deviation). The band structure calculations are performed through density functional theory based TB-LMTO-ASA approach with LDA exchange correlations. The band gap so obtained through the first principles calculations are found to be indirect types with values 1.16eV, 1.08eV, 1.50eV, and 1.29eV for MoS_2, $MoSe_2$, WS_2 and WSe_2 respectively. The density of states also supports the data come from band structure. The symmetric nature of DOS in up and down spin channels indicates all the materials are non-magnetic type. The band gap arises mainly due to contributions of hybridization between 4d states of Mo with 3s states of S and (4p) states of Se for MoS_2 and $MoSe_2$ respectively. Similarly, the band gap of WS_2 and WSe_2 arises due to contributions of hybridization between 5d states of Mo with 3s states of S and (4p) states of Se. The potential and charge distribution plot shows the supporting nature with each other. Finally charge density plot shows covalent nature of bond between M-X in (100) plane. Mixed kinds of bonds between M-X is found in (110) plane. However inter planer bonding are of Vander Wall's in nature.

ACKNOWLEDGEMENTS

Hydra Research Centre for Basic and Applied Sciences (HRCBAS) Nepal is acknowledged for partial support. A Mookerjee of SNBNCBS, Kolkota and N. P. Adhikari of CDP, TU are acknowledged for the computational code and discussion during the preparation of manuscript.

REFERENCES:

Agrawal, B. K. and Prakash, H. (2010). *Quantum Mechanics*, PHI Learning Private Limited, New Delhi, India.

Aksoy, R.; Yanzhang, M.; Chyu, M. C.; Ertas, A. (2006). White, X-ray diffraction study of molybdenum disulfide to 38.8 GPa. *Journal of Physics and Chemistry of Solids*, **67**: 1914.

Anisimov, V. I.; Aryasetiawan, F., and Lichtenstein, A. I. (1997). First-Principles calculations of electronic structure and spectra of strongly correlated system: The LDA+U method. *Journal of Physics: Condensed Matter*, **9**: 767.

Arslan, E.; Bulbil, E., Efeoglu, I., Lubric, S. T.; Tribol, E. (2004). Structure and Optical properties of Transition Metal Dichalcogenides (TMDs) MX_2 (M =Mo,W and X = S, Se) under High Pressure and High Temperature conditions. *Physics C: Solid State Phys.*, **47**: 218.

Boker, T.; Severin, R.; Muller, A.; Janowitz, C.; Manzke, R.; Vob, D.; Kruger, P.; Mazur, A.; Pollmann, J. (2001). Band structure of MoS_2, $MoSe_2$, and $MoTe_2$: Angle resolved photoelectron spectroscopy and ab-initio calculations. *Physical Review B*, *6***4**: 235305.

Coehoorn, R.; Haas, C.; Dijkstra, J.; Flipse, C. J. F.; de Groot, R. A. and Wold, A. (1987). Electronic structure of $MoSe_2$, MoS_2, and WSe_2. I. Band-structure calculations and photoelectron spectroscopy. *Physical Review B*, **35**: 6195.

Dean, C. R.; Young, A. F.; Meric, I.; Lee, C.; Wang, L.; Sorgenfrei, S. *et al*. (2010). Boron nitride substrates for high quality Graphene electronics. *Nature Nanotech*, **5**: 722.

Fang, H.; Chuang, S.; Chang, T. C.; Takei, K.; Takahashi, T.; Javey, A. (2012). High performance single layered WSe_2 p-FETs with chemically doped contacts. *Nano Letter*, **12**: 3788.

Finteis, T.; Hengsberger, M.; Straub, T.; Fauth, K.; Claessen, R.; Aver, P.; Steiner, P. (1997). *Physical Review B,* **55**: 10400.

Fischer, W. A. (2001). A Second Note on the Term "Chalcogen". *Journal of Chemical Education*, **78:** 1333.

Geim, A. K. and Grigorieva, I. V. (2013). Vander Wall's heterostructures. *Nature*, **499:** 419.

Gujarathia, D. N.; Solankib, G. K.; Deshpandeb, M. P.; Agarwalb, M. K. (2005). Band gap in tungsten sulphoselenide single crystals determined by the optical absorption method. *Materials Science in Semiconductor*, **8**: 576.

Kaphle, G. C., Adhikari, N. P., and Mookerjee, A. (2015). Study of spin glass behavior of disordered $Pt_XMn_{(1-X)}$ alloys: An Augmented space recursion Approach. *Advanced Science Letters*, **21** (9): 2681.

Kaphle, G. C.; Ganguly, S.; Banerjee R.; Khanal R.; Adhikari, C. M. ; Adhikari, N. P. and Mookerjee, A. (2012). Study of Magnetism in disordered Pt-Mn, Pd-Mn and Ni-Mn alloys: An augmented space approach. *Journal of Physics*, **24**: 295501.

Kasowski, R. V. (1973). Band Structure of MoS_2 and NbS_2. *Phys. Rev. Lett.*, **30**: 1175.

Kaxiras, E. (2003). *Atomic and electronic structure of the solids*. Cambridge University Press, United Kingdom.

Kohn, W. and Sham, L. J. (1965). Density Function Theory. *Physical Review*, **140**: A1133.

Kumar, S. and Schwingenschlog, U. (2015). Thermoelectric Response of Bulk and Monolayer $MoSe_2$ and WSe_2. *Chem. Mater.*, **27**: 1278.

Lamichhane, S.; Aryal, B.; Kaphle, G. C.; Adhikari, N. P. (2014). Structural and electronic properties of perovskites types Hydrides $ACaH_3$ (A = Cs and Rb). *BIBECHANA*, **13**: 94.

Lee, P. A. and Zuttel, A. (2003). Physics and Chemistry of materials with layered structures: Optical and Electrical Properties of Layered Semiconductor. *Material Today*, **6:** 24.

Mak, K. F.; Lee, C.; Hone, J.; Shan, J.; Heinz, T. F. (2010). Atomically Thin MoS_2 : A New direct-Gap Semiconductor. *Physical Review Letter*, **105**: 136805.

Mattheiss, L. F. (1973). Energy Bands for 2H-$NbSe_2$ and 2H-MoS_2. *Physical Review Letter*, **30**: 784.

Mogne, T. L.; Donnet, C.; Martin, J.; Tnock, A. and Pinard, N. M. (1994). Effect-of Pressure-and-Temperature-on-Structural Stability of MoS_2. *Journal of Applied Physics*, **12**:1998.

Pal, P.; Banerjee, R.; Banerjee, R.; Mookerjee, A.; Kaphle, G. C. *et al.* (2012). Magnetic ordering in Ni-rich Ni-Mn alloys around the multicritical point: Experiment and theory. *Physical Review* B, **85** (17): 174404.

Pandey, S.; Kaphle, G. C. and Adhikari, N. P. (2014). Electronic structure and magnetic properties of bulk elements (Fe and Pd) and ordered binary alloys (FePd and Fe_3Pd):TB-LMTO Approach. *BIBECHANA*, **11**: 60.

Parr, R. G., and Yang, W. (1989). *Density Functional Theory of atoms and molecules*. Oxford University Press, New York.

Perdew, J. P.; Burke, K. and Ernzerhof, M. (1996). Generalized Gradient Approximation made simple. *Physical Review Letter*, **77**: 3865.

Poudel, R. and Kaphle, G. C. (2016). Study of electronic and magnetic properties of Fe, Cr, FeCr and $FeCr_3$: TB-LMTO Approach. *Patan Gyan Sagar,* **2** (1): 80.

Radisavljevic, B.; Radenovic, A.; Brivio, J.; Giacometti, V. and Kis, A. (2011). Single layer MoS_2 transistors. *Nature Nanotechnology*, **6**: 147.

Rasch, J.; Stemmler, T. and Manzke, R. (2007). Electronic properties of the semiconductor $TiSe_2$. *Journal of Alloys and Compounds*, **442** (1-2): 262-264.

Reshak, A. H. and Auluck, S. (2003). Electronic and optical properties of the 1T phases of TiS_2 , $TiSe_2$, and $TiTe_2$. *Physical Review B,* **68** (24): 245113.

Reshak, A. H. and Auluck, S. (2007). The linear and nonlinear optical properties of S_X Se_{2-X} (X = 0.25, 0.5, 1.5, and 2.0). *Physica B,* **393**: 88.

Schutte, W. J.; de Boer, J. L. (1987). Crystal structures of tungsten disulfide and diselenide. *Journal of Solid State Chemistry*,**70**: 207.

Shankarai A.; Menezes, P. L.; Simhai, K. and Kailasi, S. V. (2008). *Sadhana*, **33** (3): 207.

Sharma, S.; Ambrosch-Draxl, C.; Khan, M. A.; Blaha, P.; Auluck, S. **(**1999). Optical properties of 2H-WSe_2. *Physical Review* B **60**: 8610.

Skriver, H. L. (1984). *The LMTO Method: Muffin Tin Orbitals and Electronic Structure*. Springer-Verlag, Berlin, Germany.

Wilson, J. A. and Yoffe, A. D. (1969). The transition metal dichalcogenides, discussion and interpretation of the observed optical, electrical and structural properies. *Advances in Physics*, **18 (**73): 193.

Wilson, J. A. and Yoffe, A. D. (1969). The transition metal dichalcogenides discussion and interpretation of the observed optical, electrical and structural properties. *Advances in Physics,* **18** (17): 73, 193.

Zhang, C.; Johnson, A.; Hsu, C. L.; Li, L. J.; Shih, C. K. (2014). Direct Imaging of Band Profile in Single Layer MoS_2 on Graphite: Quasiparticle Energy Gap, Metallic Edge States, and Edge Band Bending. *Nano Letter,* **14**: 2443.